LONG-TERM CREEP BEHAVIOR OF DEEP-BURIED MARBLE UNDER DIFFERENT CONFINING PRESSURES

by

Ersheng ZHA[a,b], Ru ZHANG[a,b*], Zetian ZHANG[a,b], Li REN[c], Wenju ZHANG[d], Zheqiang JIA[a,b], and Yang LIU[c]

Original scientific paper
https://doi.org/10.2298/TSCI180615078Z

[a]State Key Laboratory of Hydraulics and Mountain River Engineering, Sichuan University, Chengdu, China
[b]College of Water Resource and Hydropower, Sichuan University, Chengdu, China
[c]Key Laboratory of Deep Underground Science and Engineering (Sichuan University), Ministry of Education, Chengdu, China
[d]Southwest Municipal Engineering Design and Research Institute of China, Chengdu, China

To explore the long-term creep behavior of deep rock, the long-term tri-axial creep mechanical behavior of the rock under different confining pressures has been carried out. The results show that the instantaneous strain and creep strain of the high confining pressure specimen are significantly higher than that of the low confining pressure specimen under high deviatoric stress. By analyzing the failure characteristics of different confining pressure specimens, it is found that with the increase of the confining pressure, the creep failure characteristics of the marble transforms from tensile failure to shear failure. These research results have certain reference significance for the long-term stability analysis of the deep underground caverns.

Key words*: different confining pressures, deep-buried, marble, long-term, creep mechanical behavior*

Introduction

As the mineral resources and underground space on the surface and shallow parts of the earth are gradually drying-up, marching to the deep earth has become an inevitable trend. However, during the process of deep underground mining and construction, due to the different stress environment, the surrounding rock under deep conditions will exhibit different Mechanical characteristics from the shallow surrounding rock [1], such as high in-situ stress, large deformation and volume expansion [2, 3]. These characteristics make it difficult to assess the stability of the deep carven.

During the excavation process of the deep carven, the excavation process disturbed the in-situ stress environment of underground caverns. After the stress of the underground cavern wall is redistributed over a period of time, the stress remains constant and creep deformation occurs. The strain of the surrounding rock slowly increases with time, eventually leading to instability and destruction of the deep cavern. Therefore, studying the creep properties of the surrounding rock is of great importance for determining the stability of underground caverns.

Due to the high strength and small deformation of hard rock, the early research on the creep of rock mainly focused on soft rock. However, with the depth increase in the excavatio of

* Corresponding author, e-mail: zhangru@scu.edu.cn

underground caverns and the construction of large-scale underground projects, the creep properties of hard rock have become more and more important [4]. In the past decades, a lot of work has been done on the creep of hard rock: Costin [5] used a continuum damage model to analyze the creep and failure of Tennessee marble, Ito *et al*. [6] measured the time-dependent deflections of granite and gabbro pieces in ten years, Martin *et al*. [7] analyzed sixteen creep experiments of welded tuff in terms of static fatigue and gave the expression describe the correlation between the loading time and the differential stress, Yang *et al*. [8] investigated the temperature effects on creep of tuff and proposed a new time-dependent damage model with two stress intensity factors to describe the creep of tuff, Fujii *et al*. [9] carried out creep tests on Inada granite under confining pressure and discussed the circumferential strain behavior during creep test, Maranini *et al*. [10] studied the elastic-viscoplastic behavior of a Japanese granite rock by performing triaxial tests, at confining pressure varying from 0-40 MPa, Ma *et al*. [11] studied the creep characteristics of welded tuff under uniaxial compression and discovered that the transient creep for all the stress levels can be well described by power functions, and Hashiba *et al*. [12] tested the ToKi granite to quantitatively reveal the close relations between the time-dependent behaviors.

A large number of studies [13-16] have shown that rock creep is a reflection of time accumulation, and the loading time has a great influence on the creep behavior of rocks. Due to factors such as money and time, the single-stage loading time of the current research for hard rock creep tests is usually below 24 hours, and the single-stage deformation is relatively small, which makes it difficult to reflect the creep Mechanical behavior of hard rock under deep conditions.

The aim of this article is to carried out the long-term triaxial creep test of deep marble (2400 m depth) under different confining pressures. With a single-stage loading time of 5 days and the total loading time of about one month, the test analyzes the differences between the axial strain-time curve, axial strain value, steady-state creep strain rate and the accelerating creep characteristics of deep-buried marble under different confining pressures, and explored the failure characteristics and mechanisms of rock creep under different confining pressures.

Testing information

Testing specimens and apparatus

The marble selected in this article was taken from the second-level diversion tunnel of China Jinping Underground Laboratory (CJPL) at a depth of 2400 m. The marble is white and the color is pure, the main mineral is dolomite and is about 85-90% of the content. The rest of the components are calcite and quartz. Microscopic tests show that the internal structure is dense with a small number of micro-cracks. According to the advice from ISRM, cylindrical standard specimens of Ø50 mm × 100 mm were selected for the long-term triaxial creep test under different confining pressures. The specimens' information is shown in fig. 1 and tab. 1.

The creep test was performed by the large-scale program-controlled servo triaxial rheology apparatus at Sichuan University. This apparatus can perform multi-stage of single and triaxial creep tests on various types of rock materials. This apparatus can accomplish the creep

Table 1. Details of the specimens

Sample No.	Height [mm]	Diameter [mm]	Density [gcm^{-3}]	Confining pressure σ_3 [MPa]
13-59-7	100.11	49.86	2.79	6.3
13-17-3	100.22	49.62	2.82	9.6

test of axial load 0 ~ 60 tonne and confining pressure 0 ~ 30 MPa. During the creep test, the axial strain of the specimen was measured by a Mechanical dial indicator with an accuracy of 0.0001 mm and machine displacement with an accuracy of 0.001 mm to automatically collect the records.

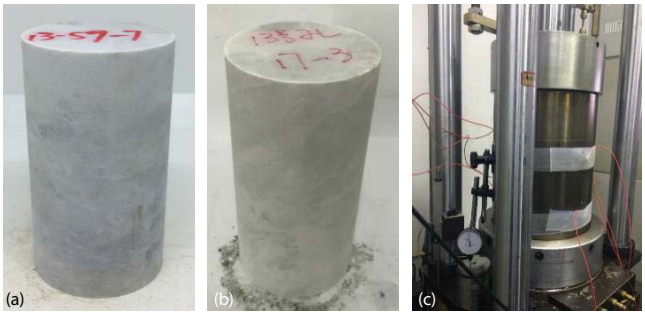

Figure 1. Specimens and apparatus for long-term; (a) specimen for σ_3 = 6.3 MPa tri-axial creep experiments, (b) specimen for σ_3 = 9.6 MPa, and (c) testing apparatus

Testing method

In this paper, the step-wise loading method was adopted. The test scheme is shown below. At the beginning of the experiment, the confining pressure was first applied to the sample. The different confining pressures applied for samples were 6.3 MPa and 9.6 MPa at 3 MPa per minute, respectively. Then, the axial pressure was applied to the initial stress state at 30 kN per minute. After 96 hours for initial pressure state maintenance, the step-wise loading was performed. The axial pressure applied at the step-wise loading stage was determined by the expected strength estimated from the conventional tri-axial tests with marble under the same confining pressure (σ_3 = 6.3 and σ_3 = 9.6). Then a certain ratio of the expected CTC strength is loaded at 30 kN per minute and maintained for 5 days in the axial direction. If the specimen is not damaged, the loading stress is increased to the next level until the specimen is destroyed.

According to the test scheme, the testing steps are: apply the confining pressure at 3 MPa per minute to the predetermined value (6.3 MPa, 9.6 MPa), apply the axial pressure at 30 kN per minute to the initial state, and maintain the constant stress state for 96 hours, apply the axial step-wise loading at 30 kN per minute, and maintain the stress for 5 days after the loading is completed to ensure that the deformation rate is stable. If the specimen is not damaged at the current stress level, the stress is increased to the next level until the specimen's failure. The deviatoric stress σg at each loading stage is shown in tab. 2.

Table 2. Step-wise loading stress $\sigma_g = \sigma_1 - \sigma_3$

Confining pressure σ_3 [MPa]	Initial state [MPa]	Step-wise loading stress σ_g [MPa]				
		1	2	3	4	5
6.3	48.3	135.9	146.3	150.8	167.2	177.7
9.6	73.6	110	132	154	165	176

Result and analysis

Axial strain-time curve characteristics

By analyzing the axial deformation of marble during loading and creep process, the step-wise loading creep curve is plotted, as shown in fig. 2.

It can be seen that the axial deformation of the long-term creep of marble under different confining pressure transits from the steady creep stage to the unsteady creep stage, and finally the accelerating creep stage with the increase of the axial pressure. The marble specimen exhibits instantaneous deformation, initial creep stage, stable creep stage, steady-state creep stage under step-wise loading, and the accelerating creep occurs at the final stress stage.

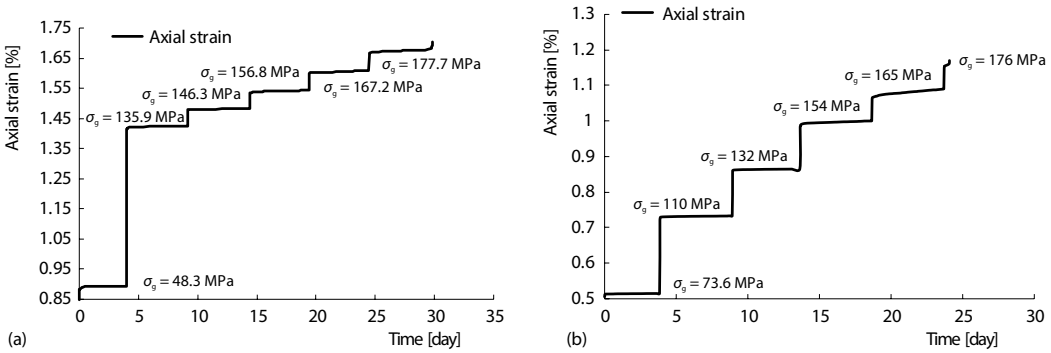

Figure 2. Axial strain-time curves of rock under different confining pressure; (a) σ_3 = 6.3 MPa, (b) σ_3 = 9.6 MPa

Axial strain

The axial deformation of the specimen under constant load consists of instantaneous deformation and creep deformation. The total strain ε_t of rock obtained by the creep test can be expressed:

$$\varepsilon_t = \varepsilon_i + \varepsilon_c \tag{1}$$

where ε_t is the total axial strain, ε_i – the instantaneous axial strain, and ε_c – the creep axial strain. The deformation of marble in the long-term creep test under different confining pressure before the accelerating creep stage is shown in figs. 3(a) and 3(b).

It can be seen from the figure that the instantaneous strain of marble under different confining pressures decreases with the increase of the deviatoric stress, fig. 3(a). This is because when the deviatoric stress is low, the instantaneous strain of the specimen is mainly composed of the elastic deformation of the matrix and the compaction of the micro-cracks. When the deviatoric stress is high (σ_g > 150 MPa), the original micro-cracks and pores inside the marble are mostly compacted. The instantaneous strain of the marble is mainly composed of the elastic deformation induced by loading. Therefore, at high stress levels, the single-stage instantaneous strain produced by marble becomes approximately proportional to the applied differential deviatoric stress.

In addition, the creep strain of marble under different confining pressures exhibits a *fall-rise* trend with the increase of the deviatoric stress, fig. 3(b). This is because when the deviator stress is low, the differences of the original micro-cracks and the physical properties of the specimen have an influence on the creep strain of the specimen. However, when the deviatoric stress is high (σ_g > 150 MPa), the creep strain shows an exponential growth trend with the increase of the deviatoric stress. The internal damage of the specimen accumulates and the micro-cracks gradually expand.

Comparing figs. 3(a) and 3(b), it can be found that with the increase of the confining pressure, the instantaneous strain and creep strain under high deviatoric stress condition of the 9.6 MPa confining pressure specimen are remarkable higher than those of the 6.3 MPa confining pressure specimen. At the stress level before the accelerating creep stage, the single-stage instantaneous strain of the 9.6 MPa confining pressure specimen is 1.15 times than that of the 6.3 MPa confining pressure specimen, while the creep strain of the 9.6 MPa confining pressure specimen reaches 1.74 times than that of the 6.3 MPa confining pressure specimen. This is consistent with the large deformation trend of rocks under deep conditions of high in-situ stress.

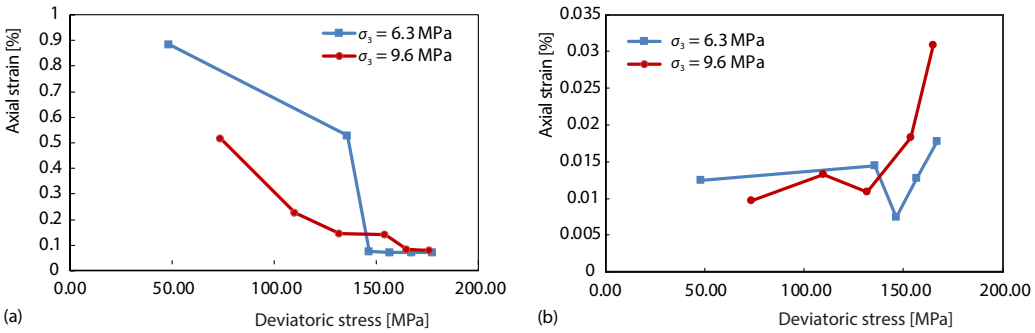

Figure 3. Axial strain for each creep stage before the accelerating creep stage; (a) instantaneous strain, (b) creep strain

Steady-state creep strain rate

The change of creep rate plays a crucial role in determining the stability of rock mass. Table 3 shows the variation trend and value of the creep rate of marble at different confining pressures. It can be seen that the creep rate at different confining pressures show an upward trend with the increase of the deviatoric stress. The steady-state creep strain rate of marble is very low under low deviatoric stress state, in the order from $10^{-8}/h^{-1}$ to $10^{-6}/h^{-1}$, tab. 3, and the influence of the confining pressure on the creep rate is not obvious. However, with the increase of the deviatoric stress, the growth rate of the steady-state creep strain rate of the 9.6 MPa confining pressure specimen is significantly higher than that of the 6.3 MPa confining pressure specimen, exhibiting an explosive growth at the accelerating creep stage. Comparing the steady-state creep strain rate of marble under different confining pressures in tab. 3, it can be found that the creep rate of the 6.3 MPa confining pressure specimen under high deviatoric stress is about 3.34 times than that of the low deviatoric stress, while the creep rate of the 9.6 MPa confining pressure under high deviatoric stress reaches 40.31 times than that of the similar low deviatoric stress. Under similar high deviatoric stress conditions, the steady-state creep strain rate of the 9.6 MPa confining pressure specimen is 10.20 times than that of the 6.3 MPa confining pressure specimen.

Table 3. Steady-state creep strain rate under different confining pressure

σ_3 = 6.3 MPa		σ_3 = 9.6 MPa	
Deviatoric stress [MPa]	Steady-state creep strain rate [h^{-1}]	Deviatoric stress [MPa]	Steady-state creep strain rate [h^{-1}]
135.90	$8.71766 \cdot 10^{-8}$	110.00	$1.01368 \cdot 10^{-7}$
146.30	$1.15824 \cdot 10^{-7}$	132.00	$7.36377 \cdot 10^{-8}$
156.80	$1.47469 \cdot 10^{-7}$	154.00	$2.60976 \cdot 10^{-7}$
167.20	$2.50842 \cdot 10^{-7}$	165.00	$6.00206 \cdot 10^{-7}$
177.70	$2.91072 \cdot 10^{-7}$	176.00	$2.96838 \cdot 10^{-6}$

Accelerating creep stage

Unsteady creep occurs in rocks under high deviatoric stress conditions. As the strain rate is greater than zero, the steady-state creep stage enters the accelerated creep stage when the strain reaches a certain degree. The creep strain rate increases and the deformation rapidly

develops, leading to the failure of rock. Figure 4 shows the axial strain and transient axial strain rate curves of the specimens at the final stress level under different confining pressures. It can be seen from the figure that the axial strain-time curves of the specimen under different confining pressures at the last loading stage show three-stages of initial creep stage, steady-state creep stage and accelerating creep stage, and the transient creep rate shows U-type of growth with the increase of time. However, the difference is that the time required for the 9.6 MPa confining pressure specimen to enter the accelerating creep stage is significantly shorter than the 6.3 MPa confining pressure specimen. Before entering the accelerating creep stage, the steady-state creep strain rate is higher, and the transient creep rate of the 9.6 MPa confining pressure specimen after entering the accelerated creep stage is also higher, which is approximately 2.5 times of the 6.3 MPa confining pressure specimen.

It can be seen in fig. 4(a) that it costs more than 5 days for the specimen to enter the accelerating creep stage, which shows that the long-term creep study of marble can more accurately reflect the creep mechanical behavior of marble.

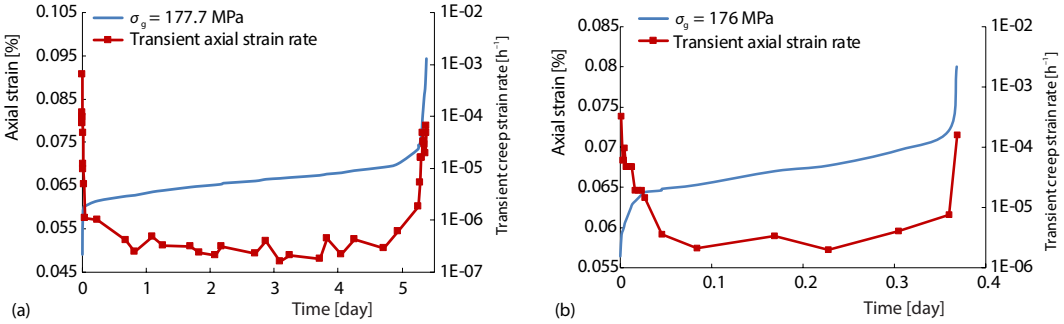

Figure 4. Axial strain and transient axial strain rate at accelerating creep stage; (a) σ_3 = 6.3 MPa, (b) σ_3 = 9.6 MPa

Failure characteristics and mechanism

The damage characteristics of long-term creep of marble under different confining pressures are shown in fig. 5. The results show that two specimens under different confining pressures both show micro-drums at destruction, which results in obvious lateral expansion. However, the failure modes of creep under different confining pressures are significantly different. The failure mode of the 6.3 MPa confining pressure specimen is the axial tensile fracture, with various kinds of tensile cracks strongly developed. The angle between the tensile rupture surface and the axial stress direction is very small, and is basically at a nearly parallel state. While the failure mode of the 9.6 MPa confining pressure specimen is complex. The axial tensile fracture and X-type conjugate shear failure exhibit at the same time, especially at the intersection of conjugate shear zones where various types of

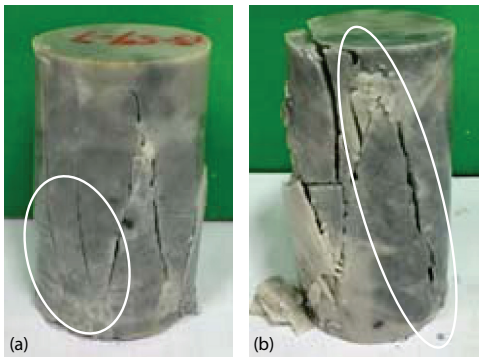

Figure 5. Axial strain and transient axial strain rate for accelerate creep stage; (a) σ_3 = 6.3 MPa, (b) σ_3 = 9.6 MPa

cracks develop strongly. The tensile rupture surface is basically parallel to the axial stress direction, and the surface of the specimen is severely peeled off after failure.

This phenomenon indicates that for creep tests of the same kind of rock, the change in confining pressure will result in different stress states and failure characteristics. Under the condition of low confining pressure, the creep failure of the specimen is dominated by the axial pressure. The pressure stress at the end of the specimen is concentrated to generate compression cracks. As the confining pressure increases, the creep failure of the specimen will be caused by axial pressure and confining pressure together. The failure mode of the sample is transformed from the single tensile failure to the tensile shear failure coexistence, and eventually transformed into the shear failure trend.

Conclusions

In this work, the long-term tri-axial creep mechanical behavior under different confining pressures of Jinping marble at 2400 m depth has been studied. It is found that the creep mechanical behaviors of marble under different confining pressures are quite different. As the confining pressure rises, the steady-state creep strain rate and the creep strain are significantly increased, and the steady-state creep strain rate also has a significant increase before entering the accelerating creep stage. Before entering the accelerating creep stage, the single-stage instantaneous strain of the high confining pressure specimen is 1.15 times than that of the low confining pressure specimen, while the creep strain of the high confining pressure specimen reaches 1.74 times of the low confining pressure specimen. Under similar high deviatoric stress conditions, the steady-state creep strain rate of the high confining pressure specimen is 10.20 times than that of the low confining pressure specimen. The transient creep rate of the high confining pressure specimen is approximately 2.5 times of the low confining pressure specimen when entering the accelerating creep stage. The value of confining pressure will directly affect the failure characteristics of creep. The main failure mode of the low confining pressure specimen is the compression crack induced by the stress concentratio at the end of the specimen. With the confining pressure rises, the trend of damage characteristics transits to tensile shear failure coexistence, and eventually transforms into the shear failure under high confining pressure condition. This indicates that under the deep underground conditions of high in-situ stress, the creep mechanical behavior of rock will be very different from the shallow conditions. The steady-state creep strain rate and the creep strain are increased significantly, and the steady-state creep strain rate is also significantly increased. Besides, the rock failure behavior transforms from the single tensile failure to the shear failure. The research shows that it will be more challenging to build deep underground projects. This problem needs to be given sufficient attention.

Acknowledgment

This work was supported by the National Science Foundation for the Excellent Youth Scholars (No. 51622402), the Youth Science and Technology Innovation Research Team of Sichuan Province (No. 2017TD0007) and the National Science Foundation (No. 51804204).

Nomenclature

Greek symbols

ε_c – creep axial strain, [–]
ε_i – instantaneous axial strain, [–]
ε_t – total axial strain, [–]
σ_g – deviatoric stress, [MPa]
σ_1 – major principle stress, [MPa]
σ_3 – minor principle stress, [MPa]

References

[1] Manchao, H., *Present Situation and Prospect of Rock Mechanics in Deep Mining Engineering*, Science Press, Beijing, 2004
[2] Manchao, H., *et al.*, Coupled Supporting Mechanical Principle of Soft Rock Roadways and Its Application, *Hydrogeology & Engineering Geology*, *2* (1998), 2, pp. 1-4
[3] Jiang, Y. D., *et al.* Research on Floor Heave of Roadway in Deep Mining, *Chinese Journal of Rock Mechanics & Engineering, 14* (2004), 23, pp. 2396-2401
[4] Brantut, N., *et al.*, Time-Dependent Cracking and Brittle Creep in Crustal Rocks: A review, *Journal of Structural Geology*, *52* (2013), 5, pp. 17-43
[5] Costin, L. S., Time-Dependent Damage and Creep of Brittle Rock, *Proceedings*, 2 Session Sponsored by the Engineering Mechanics Division of the American Society of Civil Engineers in Conjunction with the ASCE Convention, Detroit, Mich., USA, 1985, pp. 25-38
[6] Ito, H., *et al.*, A Ten Year Creep Experiment on Small Rock Specimens, *International Journal of Rock Mechanics & Mining Sciences & GeoMechanics Abstracts*, *24* (1987), 2, pp. 113-121
[7] Martin, R. J., *et al.*, Creep and Static Fatigue of Welded Tuff from Yucca Mountain, Nevada, *International Journal of Rock Mechanics & Mining Sciences*, *34* (1997), 3-4, pp. 190-191
[8] Yang, C., *et al.*, Temperature Effects on Creep of Tuff and Its Time – Dependent Damage Analysis, *International Journal of Rock Mechanics & Mining Sciences*, *34* (1997), 3-4, pp. 383-384
[9] Fujii, Y., *et al.*, Circumferential Strain Behavior during Creep Tests of Brittle Rocks, *International Journal of Rock Mechanics & Mining Sciences*, *36* (1999), 3, pp. 323-337
[10] Maranini, E., *et al.*, A Non-Associated Viscoplastic Model for the Behaviour of Granite in Triaxial Compression, *Mechanics of Materials*, *33* (2001), 5, pp. 283-293
[11] Ma, L., *et al.*, An Experimental Study on Creep of Welded Tuff, *International Journal of Rock Mechanics & Mining Sciences*, *43* (2006), 2, pp. 282-291
[12] Hashiba, K., *et al.*, Time-Dependent Behaviors of Granite: Loading-Rate Dependence, Creep, and Relaxation, *Rock Mechanics & Rock Engineering*, *49* (2016), 7, pp. 2569-2580
[13] Fabre, G., *et al.*, Creep and Time-Dependent Damage in Argillaceous Rocks, *International Journal of Rock Mechanics & Mining Sciences*, *43* (2006), 6, pp. 950-960
[14] Tsai, L. S., *et al.*, Time-Dependent Deformation Behaviors of Weak Sandstones, *International Journal of Rock Mechanics & Mining Sciences*, *45* (2008), 2, pp. 144-154
[15] Li, Y., *et al*., Time-Dependent Tests on Intact Rocks in Uniaxial Compression, *International Journal of Rock Mechanics & Mining Sciences*, *37* (2000), 3, pp. 467-475
[16] Nadimi, S., *et al*., Triaxial Creep Tests and Back Analysis of Time-Dependent Behavior of Siah Bisheh Cavern by 3-D Distinct Element Method, *Tunneling and Underground Space Technology*, *26* (2011), 1, pp. 155-162

Paper submitted: June 15, 2018
Paper revised: August 20, 2018
Paper accepted: September 15, 2018